



National Library of Canada

Cataloguing Branch
Canadian Theses Division

Ottawa, Canada
K1A 0N4

Bibliothèque nationale du Canada

Direction du catalogage
Division des thèses canadiennes

NOTICE

The quality of this microfiche is heavily dependent upon the quality of the original thesis submitted for microfilming. Every effort has been made to ensure the highest quality of reproduction possible.

If pages are missing, contact the university which granted the degree.

Some pages may have indistinct print especially if the original pages were typed with a poor typewriter ribbon or if the university sent us a poor photocopy.

Previously copyrighted materials (journal articles, published tests, etc.) are not filmed.

Reproduction in full or in part of this film is governed by the Canadian Copyright Act, R.S.C. 1970, c. C-30. Please read the authorization forms which accompany this thesis.

**THIS DISSERTATION
HAS BEEN MICROFILMED
EXACTLY AS RECEIVED**

AVIS

La qualité de cette microfiche dépend grandement de la qualité de la thèse soumise au microfilmage. Nous avons tout fait pour assurer une qualité supérieure de reproduction.

S'il manque des pages, veuillez communiquer avec l'université qui a conféré le grade.

La qualité d'impression de certaines pages peut laisser à désirer, surtout si les pages originales ont été dactylographiées à l'aide d'un ruban usé ou si l'université nous a fait parvenir une photocopie de mauvaise qualité.

Les documents qui font déjà l'objet d'un droit d'auteur (articles de revue, examens publiés, etc.) ne sont pas microfilmés.

La reproduction, même partielle, de ce microfilm est soumise à la Loi canadienne sur le droit d'auteur, SRC 1970, c. C-30. Veuillez prendre connaissance des formules d'autorisation qui accompagnent cette thèse.

**LA THÈSE A ÉTÉ
MICROFILMÉE TELLE QUE
NOUS L'AVONS REÇUE**

CONSTRAINED CAVITATING FLOW PAST SIMPLE
BOUNDARY ELEMENTS

Noor Azar Salman

A Dissertation

in

The Faculty

of

Engineering

Presented in Partial Fulfillment of the Requirements
for the degree of Master of Engineering at
Concordia University
Montreal, Quebec, Canada

September 1978



Noor Azar Salman, 1978

ABSTRACT

ABSTRACT

CONSTRAINED CAVITATING FLOW PAST SIMPLE BOUNDARY ELEMENTS

Noor Azar Salman

A development project was undertaken to design a test set up to study the characteristics of noise and vortex shedding frequency related to constrained cavitating flow past simple boundary elements. The boundary element for which the forebody was streamlined is arbitrarily designated as the element set in the normal orientation. The boundary element with the vertical front face is designated as the element set in the reversed orientation.

The present studies indicate that the gap velocity U_1 is the proper velocity scale to normalise the vortex shedding frequency for flow past the boundary elements set in the normal orientation. The preliminary results also indicate that the noise radiated by cavitating flow past the boundary elements set in the reverse orientation attain a peak value (RMS) in a narrow band of cavitation numbers for all blockages tested.

ACKNOWLEDGEMENTS

ACKNOWLEDGEMENTS

The author wishes to express his appreciation to Dr. A.S. Ramamurthy for suggesting the development project related to constrained flow past cavitating boundary elements.

The assistance of Dr. P. Bhaskaran during the course of the project is gratefully acknowledged. Thanks are also due to Messes. L. Stankevicius, D. Roy, Ernest, and the members of the machine shop for their assistance.

TABLE OF CONTENTS

TABLE OF CONTENTS

	PAGE
ABSTRACT	i
ACKNOWLEDGEMENT	ii
LIST OF FIGURES	v
LIST OF TABLES	v
NOMENCLATURE	vi
 CHAPTER I INTRODUCTION	
1.1 General Remarks	1
1.2 Hydrodynamic Characteristics of Flow Past Boundary Elements	1
1.3 Vortex Shedding Frequency	2
1.4 Blockage Effects	3
1.4.1 Non-cavitating sources	3
1.4.2 Cavitating sources	4
 CHAPTER II EXPERIMENTAL SET-UP	6
 CHAPTER III ANALYSIS OF RESULTS	
3.1 Boundary Elements (Normal Orientation)	9
3.2 Boundary Elements (Reversed Orientation)	10
3.2.1 Vortex Shedding Data	10
3.2.2 Noise Test Data	12
 CHAPTER IV CONCLUSIONS AND SUGGESTIONS	
4.1 Conclusions	14
4.2 Suggestions	15

(continued)

PAGE

REFERENCES	16
APPENDIX I - FIGURES	19
APPENDIX II - TABLE	19

LIST OF FIGURES AND TABLE

LIST OF FIGURES

FIGURE	DESCRIPTION	PAGE
1	Venturi Apparatus	19
2	Cavitating Boundary Elements	20
3	Modified Test Section	21
4	Instrumentation	22
5	Test Section for Noise and Erosion Tests (modified test section)	23
6	Variation of Strouhal Number With Cavitation Number, Boundary Element (normal orientation)	24
7	Variation of Strouhal Number With Blockage (non cavitating) and Cavitation Number, Boundary Element (normal orienta- tion)	25
8	Variation of Strouhal Number With Cavitation Number, Boundary Element (reversed orientation)	26
9	Pressure Records, Boundary Element (reversed orientation)	27
10	Typical Power Density Spectra Boundary Element (reversed orientation) $b/B = .33$	28
11	Variation of S_1 with σ_1 for Boundary Element (normal orientation)	29
12	Strouhal Number of Vortex Formation for Boundary Element (normal orientation)	30
13	Noise Spectra for Different Cavitation Numbers at Constant Velocity, Boundary Element (reversed orientation)	31

FIGURE	DESCRIPTION	PAGE
14	Sound Pressure Level at Different Velocities and Cavitation Numbers, Boundary Element	32

LIST OF TABLES

TABLE	DESCRIPTION	PAGE
1	Comparison of Data	33

NOMENCLATURE

NOMENCLATURE

b	source size (width)
B	width of test section
B/b	blockage (constraint)
C_c	contraction coefficient
f	frequency of vortex shedding
P	pressure in undisturbed approaching flow
P_v	vapor pressure
R	Reynolds number (Ub/ν)
S	Strouhal number normalized by U ($= fb/U$)
S_1	Strouhal number normalized by U_1 ($= fb/U_1$)
SPL	sound pressure level (dB) $= 20 \log_{10} (P/P_{ref})$
U	mean velocity of undisturbed approaching flow
U_1	mean gap velocity (Fig. 3)
U_j	contracted jet velocity (Fig. 3)
U_s	velocity along the separation stream line (Fig. 3)
ω	frequency (cps) in noise spectra
ν	kinematic viscosity
ρ	density of fluid
σ	cavitation number $(P-P_v)/\frac{1}{2} \rho U^2$
σ_1	cavitation number $(P-P_v)/\frac{1}{2} \rho U^2$

(continued)

INTERRELATIONS

$$k = U_s/U = \frac{B}{C_c(B-b)} \quad U_j = U_1/C_c \quad \sigma_1 = (1-b/B)^2 \sigma$$

$$U_1 = U/(1-b/B)$$

$$S_1 = (1-b/B)S$$

CHAPTER I
INTRODUCTION

1

J

CHAPTER I
INTRODUCTION

1.1 GENERAL REMARKS

When the local pressure in flowing liquid is sufficiently lowered either by increasing the ambient velocity or by decreasing the ambient pressure, a fully developed cavity attached to a solid boundary occurs. This characteristic of the flow is generally determined, to a large extent, by σ .

The ratio of model area to the test section area is denoted as blockage and it determines the influence of the side walls on the characteristics of flow. Some studies have been made in the past, to understand the effects of blockage on the wake produced by flow passing over boundary elements under cavitating conditions [1,2,3].

The present effort is principally concerned with the development of a set-up to study the effects of blockage on the vortex shedding frequency and noise associated with cavitating flow past boundary elements set on the wall of a two-dimensional venturi set up.

1.2 HYDRODYNAMIC CHARACTERISTICS OF FLOW PAST
ROUGHNESS ELEMENTS

Some studies have been made [1,2] on the hydrodynamic

characteristics of flow past a boundary element mounted on the walls of water tunnels. These studies were aimed at determining the effect of blockage on Strouhal number for flow past a boundary element [1,2] mounted in water tunnels (Fig.1). However, in the results reported, partly streamlined boundary elements (Fig. 2) were used and consequently, the test condition often spanned the critical Reynolds number. This, in turn, rendered the results to be highly Reynolds number dependent. The experimental results of Arndt [23] indicate that the cavitation inception index is directly related to the skin friction coefficient for both smooth and rough boundary element.

1.3 VORTEX SHEDDING FREQUENCY

Vigander [2] used high speed photography to obtain the vortex shedding frequency for flow past boundary elements, shown in Fig. 2(a). He states that "the intensity of pressure fluctuations at the vortex shedding frequency decreases in the downstream direction. This decrease represents the decay of the vortices as they are convected downstream." He also states that cavitation in the quasi-steady region reduces the frequency of vortex shedding formation to one-half the frequency of vortex formation in non-cavitating flow. Appel [1] has made some studies related to the effects of blockage on vortex shedding. According to him the vortex shedding frequency related to flow past a rigid gate housed in a conduit

is different from that of the flow past a spring mounted gate. The latter gives rise to hydroelastic vibration which is controlled by the elastic characteristics of the gate. For the rigid gate, he observed that the eddy behind the gate is stable.

For flow past a normal plate subject to constrained flow, Shaw [13,14] states that the ratio of the separation velocity to the uniform approach velocity, denoted by the factor k increases uniformly with B/b . Note that the variable k is related to the jet contraction coefficient C_c (see notations). He also showed that the jet contraction velocity U_j is equal to the separation velocity U_s when the blockage is at least moderate. It may be added that the contraction coefficient is a weak function of blockage for high blockage ratios.

1.4 BLOCKAGE EFFECTS

1.4.1 Non-Cavitating Sources

In water tunnel tests, the side walls of the test section can change the hydrodynamic force coefficients and the vortex shedding frequency of the model set in the test facility. Several investigations have been made to determine the effect of blockage on the drag coefficient [10,11] and Strouhal number [4,5,6,7,8] of non-cavitating bluff bodies.

It has been shown that the separation velocity U_s (Fig.3) is the characteristic velocity scale that should be

used to normalise the drag coefficient when the blockage effects are severe [5,9,10,11,12]. Further, when the configuration of the body is similar to the one shown in Fig.2(a), the contraction coefficient C_c is a weak function of blockage. As such, the gap velocity U_1 (Fig. 2(b)) can be used in place of U_s (or U_j) in normalising the vortex shedding frequency for flow past such elements.

1.4.2 Cavitating Sources

Very recently, Popp [22] has analysed the problem of wall effects in cavitating flows and his conclusions are in very good agreement with the studies of Wu et al [15,16]. Bhaskaran [18] has recently conducted an experimental study related to blockage effects on bluff bodies set in a two-dimensional test section. According to him, the gap velocity U_1 (Fig.3) and the jet contraction velocity U_j are the proper velocity scales to normalise the drag force and the vortex shedding frequency for constrained cavitating flow past bluff bodies. Earlier studies related to the vortex shedding characteristics of flow past cavitating bluff bodies include those of Syamala Rao [19], Young [20] and Hammitt [21].

The present project was undertaken to achieve the following goals:

- (1) Develop a simple test set-up which can be used to determine the characteristics of constrained cavitating flow past simple boundary elements.
- (2) Conduct preliminary tests to check the feasibility of conducting comprehensive test programs related to the following aspects of cavitating flow past boundary elements:
 - (i) vortex shedding characteristics including blockage effects
 - (ii) cavitation noise characteristics
 - (iii) cavitation erosion characteristics
- (3) Correlate data of preliminary tests related to (i) and (ii) above, and arrive at tentative conclusions.

CHAPTER II
EXPERIMENTAL SET-UP

CHAPTER II

EXPERIMENTAL SET-UP

The present investigation was carried out in the two-dimensional test section (154 mm x 6 mm) of a venturi flow apparatus which was developed for the study of flow past roughness elements mounted on the walls of the test section. One side of the test section was made of thick plexiglass to aid both stroboscopic and high speed photographic studies. Polished stainless steel roughness elements formed the basic shapes for the cavitation sources (Fig. 2). The minimum height of the model was 16 mm. The model was mounted in the test section, as shown in Fig. 3. Static pressure taps were housed in the windows of the test section and these were connected, in turn, to the manometers and pressure transducers. The flow was measured with the help of a calibrated venturimeter. The vortex shedding frequency was obtained with the help of a pressure transducer located in the edge of the wake region of the course. The location of the transducer for different sizes of the model was determined by trial and error to register the primary vortex shedding frequency. The associated instrumentation is shown in Fig. 4. The amplified signal was recorded on a strip chart recorder and the recorded signals were often checked with the help of a frequency counter. An analyser (B & K) fitted with a level recorder was used for spectral analysis of the recorded data,

especially when the frequency of vortex shedding was not discernible from direct records of the strip chart. For this purpose, large enough time samples were chosen. These large enough time samples were chosen on the time axis, in order to be able to make a representative statistical average over the entire recorded signal and that was about $\frac{400}{f}$ seconds.

Besides the larger test section (154 mm x 6 mm), a narrower test section (6 mm x 61 mm) was used to conduct an erosion test which required much larger velocities. The narrow test section was also used for the noise tests.

The noise radiated by the boundary elements was measured with the help of a noise meter (B & K). A simple parabolic-shaped device was used to house the transducer (Fig.5). The sound level meter was located at about 150 mm from the face of the test section in the horizontal plane. The sound level meter had a built-in octave filter set with eleven band pass filters in the range of 31.5 Hz to 31.5 KHz. Sound pressure levels were obtained for different cavitation numbers at fixed flow velocities.

Some tests were conducted to determine the erosion characteristics of flow past boundary elements. For this, soft aluminum test specimens were mounted in the wake region of the boundary elements. Since the number of erosion tests conducted were very few, no detailed analysis of the test results were made. Nevertheless, the soft aluminum plates

housed in the wake of the boundary elements were eroded considerably during short term (30 minutes) tests. This indicated the feasibility of using the narrow section for erosion tests.

CHAPTER III

ANALYSIS OF RESULTS

CHAPTER III
ANALYSIS OF RESULTS

3.1 BOUNDARY ELEMENTS (NORMAL ORIENTATION)

Since the Reynolds number of the flow was close to the critical Reynolds number, the vortex shedding frequency, and hence, the Strouhal numbers S display a wide scatter (Fig.6). Consequently, it is difficult to establish the dependence of S and S_1 with a cavitation number. In spite of this, mean curves were drawn to indicate the dependence of S and S_1 on the cavitation number (Figs. 6,7).

Fig. 7(a) shows the effect of blockage on the vortex shedding frequency of the boundary elements set in the normal orientation. The cavitation number of the flow was very large (non-cavitating). The modified Strouhal number S_1 was based on the gap velocity U_1 , (Fig.7), while the Strouhal number S was based on the undisturbed velocity U . The vortex shedding of these elements ceased when choking conditions prevailed. Similar observations have been made for flow past bluff bodies [18]. As a further attempt to unify the data, the modified cavitation number σ_1 was adopted to include the relationship between S_1 and σ_1 which appears to provide a nearly unique representation between these two variables for a wide range of blockage.

The mean curves denoting S_1 for the three different blockage ratios tested tend to merge into a single curve for the non-cavitating range (Fig.7(b)).

3.2 BOUNDARY ELEMENTS (REVERSED ORIENTATION)

3.2.1 Vortex Shedding Data

The relationship between cavitation number and vortex shedding frequency for flow past boundary elements set in the reversed orientation (Fig. 2(b)) is shown in Fig. 8. In these experiments, the element shape chosen eliminated Reynolds number effects (Fig.8). As before, one notices that the vortex shedding will cease when choking conditions occur. As a matter of fact, it is difficult to analyse the vortex shedding frequency in the neighbourhood of choking conditions. The spectral plots of the pressure signals were characterized by well defined peaks only when cavitation numbers were sufficiently high (Fig. 10). A sequence of pressure records for a range of cavitation numbers is shown in Figs. 9 and 10. Fig. 10 shows the corresponding spectral density plots for a few selected tests. The dip in the spectra at 63 cycles and 200 cycles in all spectral plots (Fig.10) is due to the shift registered by the level recorder as different bandwidths are scanned. As such, this dip should be ignored while interpreting the spectra. When choking conditions are approached (Fig.9), the pressure pulsations occur intermittently. Fig. 11

shows the dependence of S_1 on σ_1 . As it is shown the three curves merge to a unique curve.

It may be added that no attempt was made to provide a unified presentation of the results for the vortex shedding frequency for constrained flow past boundary elements set in the reversed orientation. To do this, one should know the value of the parameter k for flow past the boundary element in question. For the case of normal orientation, the contraction coefficient C_c was a weak function of blockage for moderately constrained flows and hence, one can use U_1 instead of U_j (see notations, page v) to unify the results. Since C_c is a strong function of b/B for the reversed orientation of the roughness elements, one cannot expect the test data to be unified when S is replaced by S_1 . Therefore, in the absence of the information about k , it is very difficult to analyze this case further. Fig. 12 shows the comparison of the vortex shedding data for constrained flow past the boundary element with some earlier results.

Generally, the present results are in good agreement with the latter, in spite of the fact that there is some difference in the element shapes. Since the experiments conducted (set in the normal orientation) are subject to the influence of Reynolds number effects, the comparison should be made only qualitatively. Table 1 shows the summary of the

comparison of results.

3.2.2 Noise Test Data

Fig. 13 shows a typical spectral distribution of sound pressure levels ($\omega = 8,000$ cps) at a fixed velocity for cavitating flow past the boundary element set in the normal orientation. Beyond the inception point, it indicates that the sound pressure levels increase with the reduction of cavitation number, reach a peak value and decrease with further reduction of cavitation number. At the inception of cavitation, the sound pressure level increases due to the formation and collapse of vapour bubbles. This is especially true in the high frequency range of the spectra, since the smaller bubbles are associated with higher frequencies. As the cavitation number is further reduced, the number of bubbles and their collapse pressure increase and this, in turn, increases the radiated sound pressure. The formation of longer cavity at lower cavitation number promotes the growth of larger bubbles at the expense of smaller ones. As the bubbles become bigger, they absorb more and radiate less noise in the higher frequency range. Hence, the rise of sound pressure levels at the high frequency band is limited, as one approaches the lower range of cavitation numbers. This also accounts for the reduction of the high frequency noise as choking conditions are approached.

Fig. 14 indicates the spectral distribution of cavitation noise for a few selected tests in which σ was varied at a fixed velocity. For this test series, the peak noise occurred when σ reached a value of 3.28. Clearly, in the low end of the spectra ($\omega < 500$ cps), an increase in noise level in all frequency bands as one decreases the cavitation number from large cavitation numbers (non-cavitating conditions).

CHAPTER IV
CONCLUSIONS AND SUGGESTIONS

CHAPTER IV
CONCLUSIONS AND SUGGESTIONS

4.1 CONCLUSIONS

Based on the present study, the following conclusions can be reached.

(1) For constrained flow past the boundary element set in the normal orientation the gap velocity U_1 is the proper velocity scale that yields a modified Strouhal number S_1 which is nearly constant over a large range of cavitation numbers. Further, the use of U_1 to form the modified cavitation number σ_1 yields a relationship between S_1 and σ_1 which is almost unique for all blockages considered in the present study.

(2) As the cavitation number is varied over a wide range for constrained cavitating flow past the boundary element set in the reversed orientation, the peak radiated noise occurs in a very narrow band of cavitation numbers.

4.2 SUGGESTIONS

Detailed studies should be made to confirm the results of preliminary studies and vortex shedding characteristics of boundary elements. As a part of this study, one should investigate the relationship between the value of k and blockage for the two boundary elements considered.

REFERENCES

REFERENCES

- [1] David W. Appel, Masce, and Charles L. Sanford, "Vibration Problems in Hydrodynamics Structures". ASCE Proceedings, J. Hydraulics Division, Vol.87, (Nov.1961).
- [2] Svein Vigander. "An Experimental Study of Wall Pressure Fluctuation in a Cavitating Turbulent Shear Flow". Report No.21, University of Kansas, (May, 1965).
- [3] Sandord, C.L., "A Study of Flow Through Abrupt Two-Dimensional Expansion. Formation of Vortices", Studies in Engineering Mechanics, Report No.7, University of Kansas.
- [4] Ivany, R.D., Hammitt, F.G., and Mitchell, I.M., "Cavitation Bubble Collapse Observation in a Venturi", Trans.ASME, Serd, (Sept. 1966), pp.649-657.
- [5] Ramamurthy, A.S., and Ng, C.P., "Effects of Blockage on Steady Force Coefficients", J. Engineering Mechanics Division, ASCE, Vol.99, No.EM4, Proc.Paper 9905, (Aug.1973), pp.755-772.
- [6] Toebe\$, G.H., "The Frequency of Oscillating Forces Acting on Bluff Cylinders in Constricted Passages". Res., Paris, (1971), 2, B-7-58.
- [7] Toebes, G.H., and Ramamurthy, A.S., "Lift and Strouhal Frequency for Bluff Shapes in Constricted Passages", Proc. Conf. on Flow Induced Vibration in Nuclear Reactors, Argonne National Laboratory, Illinois, (1970), pp.225-247.
- [8] Tozkas, A., "Effect of Confining Walls on the Periodic Wake of Cylinders and Plates. M.S.Thesis, Dept. of Eng. Mechanics and Hydraulics, University of Iowa, (1965).

- [9] Ellis, A.T., Gruber, G., and George, N., "An Experimental Investigation of Shock Wave-Bubble Interaction and Reflection Holograms of Long Polymer Molecules", Calif.Inst.Tech., Eng. and Appl.Science, Rep.E-115-A.1, (1968).
- [10] Fitzpatrick, H.M., and Strasberg, M., "Hydrodynamic Sources of Sound", (1956), 2nd Symp. Naval Hydrodyn., Washington, D.C., pp.241-280.
- [11] Ramamurthy, A.S., and Lee, P.M., "Wall Effects of Flow Past Bluff Bodies", J. Sound and Vibration, (1973), 31(4); pp.443-451.
- [12] Birkhoff, G., Plesset, M., and Simmons, N., "Wall Effects in Cavity Flow", Part 1, Quarterly of Applied Mathematics, Vol.8, No.2, (1950), pp.151-168; Part 2, Vol.9, No.4, (1952), pp.413-421.
- [13] Shaw, T.L., "Steady Flow Past Plate in Channel", J. Hydraulic Div., Proc. ASCE, Hy.6, (1969), No.6903, pp.2013-2028.
- [14] Shaw, T.L., "Effect of Side Walls on Flow Past Bluff Bodies", J. Hydraulic Div., Proc. ASCE, Hy.1, (Jan.1971), No.7788, pp.65-79.
- [15] Wu, T.Y., Whitney, A.K., and Lin, J.D., "Wall Effects in Cavity Flows", Calif.Inst. of Tech. Pasadena, Calif., E-111, A.5, (Aug.1969).
- [16] Wu, T.Y., Whitney, A.K., and Brennen, C., "Cavity Flow Wall Effects and Correction Rules". J. Fluid Mechanics 49,2, (1971), pp.223-256.
- [17] Rangaswami Narayanan, "Theoretical Analysis of Flow Past Leaf Gate", Proc. ASCE, Hydraulic Division, (June, 1972).

- [18] Bhaskaran, P., D.Eng.Thesis, Concordia Univ.(1976).
Montreal, Canada.
- [19] B.C.Sayamalrao and N.S. Lakshmana Rao, Department of Civil Engineering, Indian Institute of Science, Bangalore 560,012, India.
- [20] Yong, J.O., and Holl, J.W., "Effects of Cavitation on Periodic Wakes Behind Symmetric Wedges", J.Basic Engineering, Trans. ASME, (March,1966), pp.163-176.
- [21] Hammitt, F.G., and Kemppainen, D.J., "Cavitation Flow Past Transverse Cylinder in Venturi Diffuser With Water and Mercury". Proc.Third Conf. on Fluid Mechanics and Fluid Machinery, Budapest, (Sept.1969), pp.255-265.
- [22] Popp, S., "Theoretical Investigations and Numerical Evaluations of Wall Effects in Cavity Flows", J.Fluids Engineering, Trans. ASME, (Dec.1975), Vol.97, No.4, pp.482-491.

APPENDIX I

FIGURES

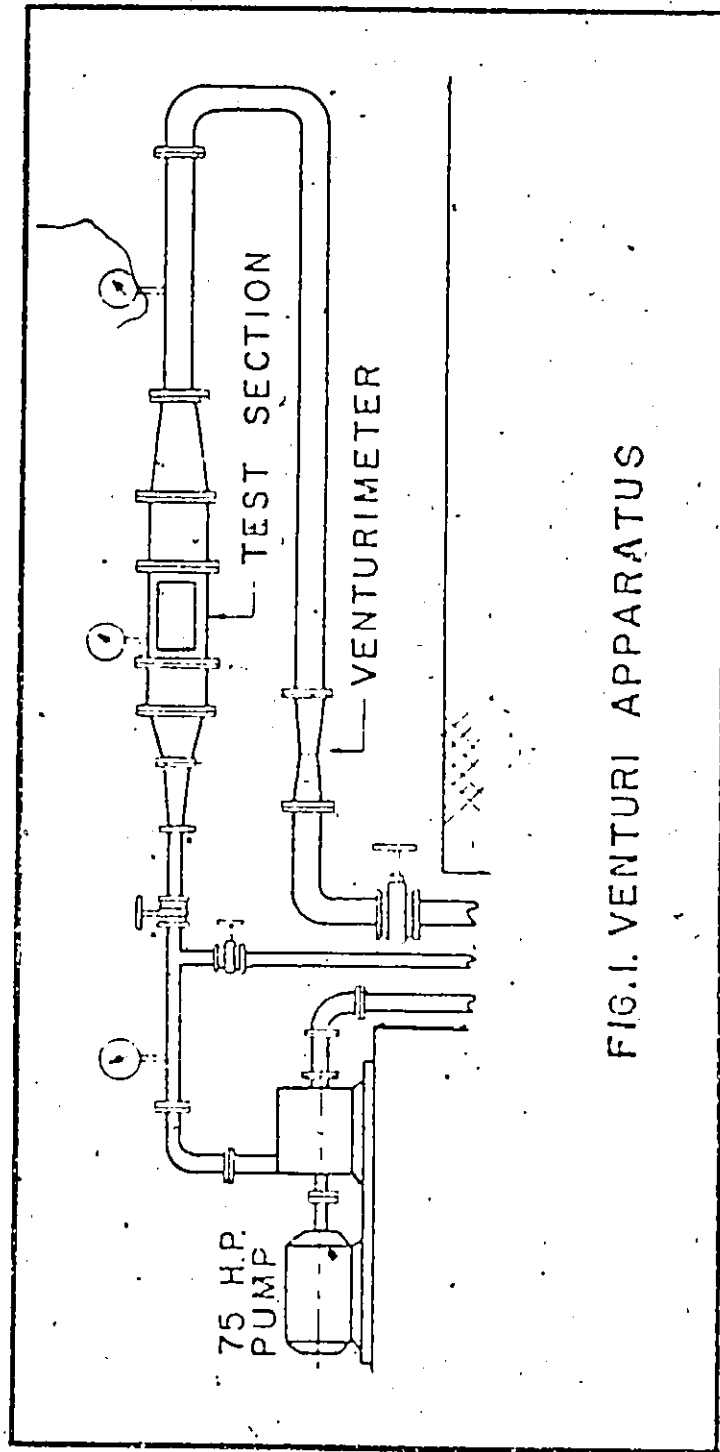
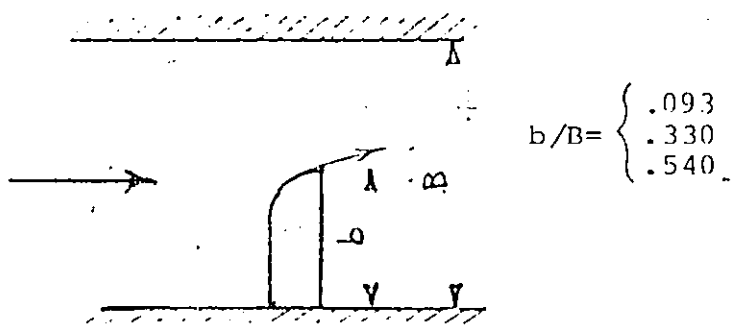
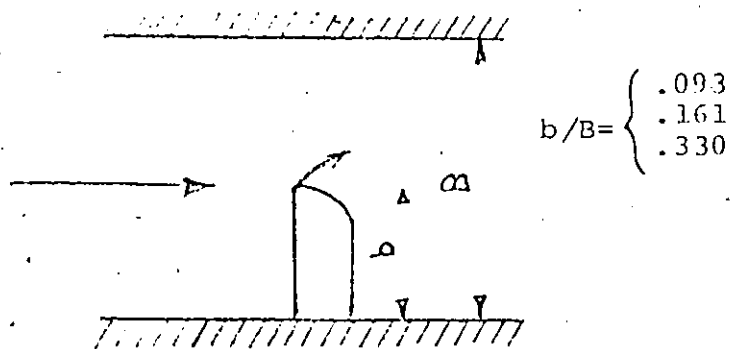


FIG. I. VENTURI APPARATUS



a) NORMAL ORIENTATION



b) REVERSED ORIENTATION

FIGURE 2 - CAVITATING BOUNDARY ELEMENTS

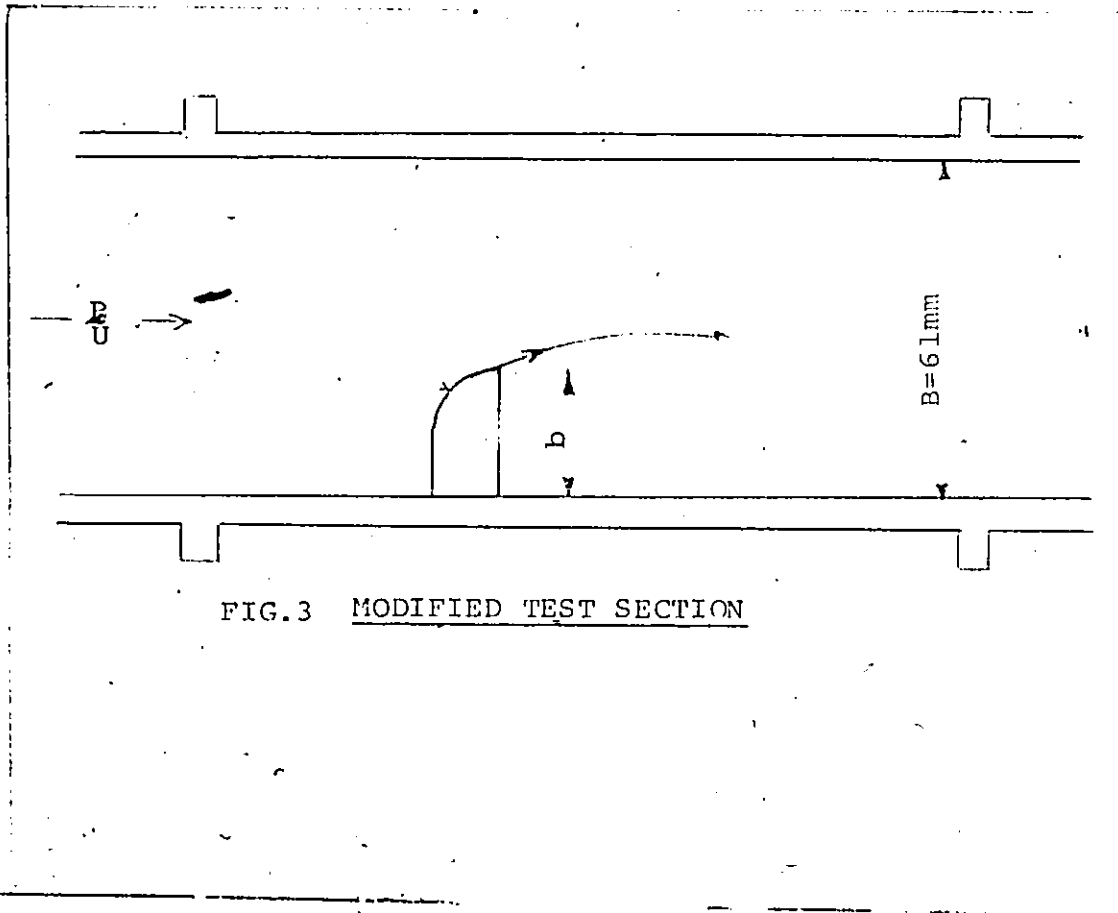


FIG. 3 MODIFIED TEST SECTION

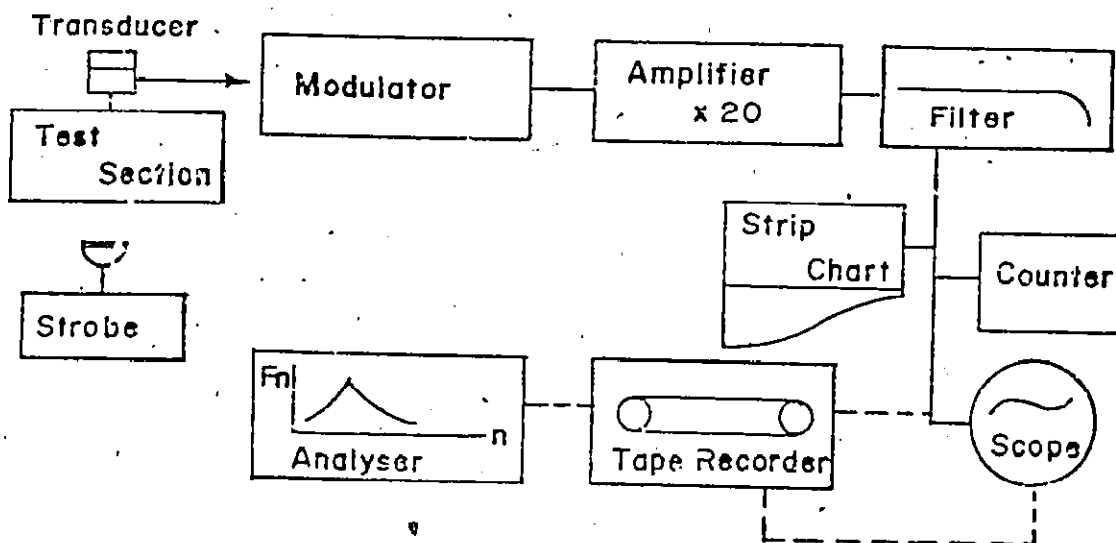


FIG. 4 INSTRUMENTATION

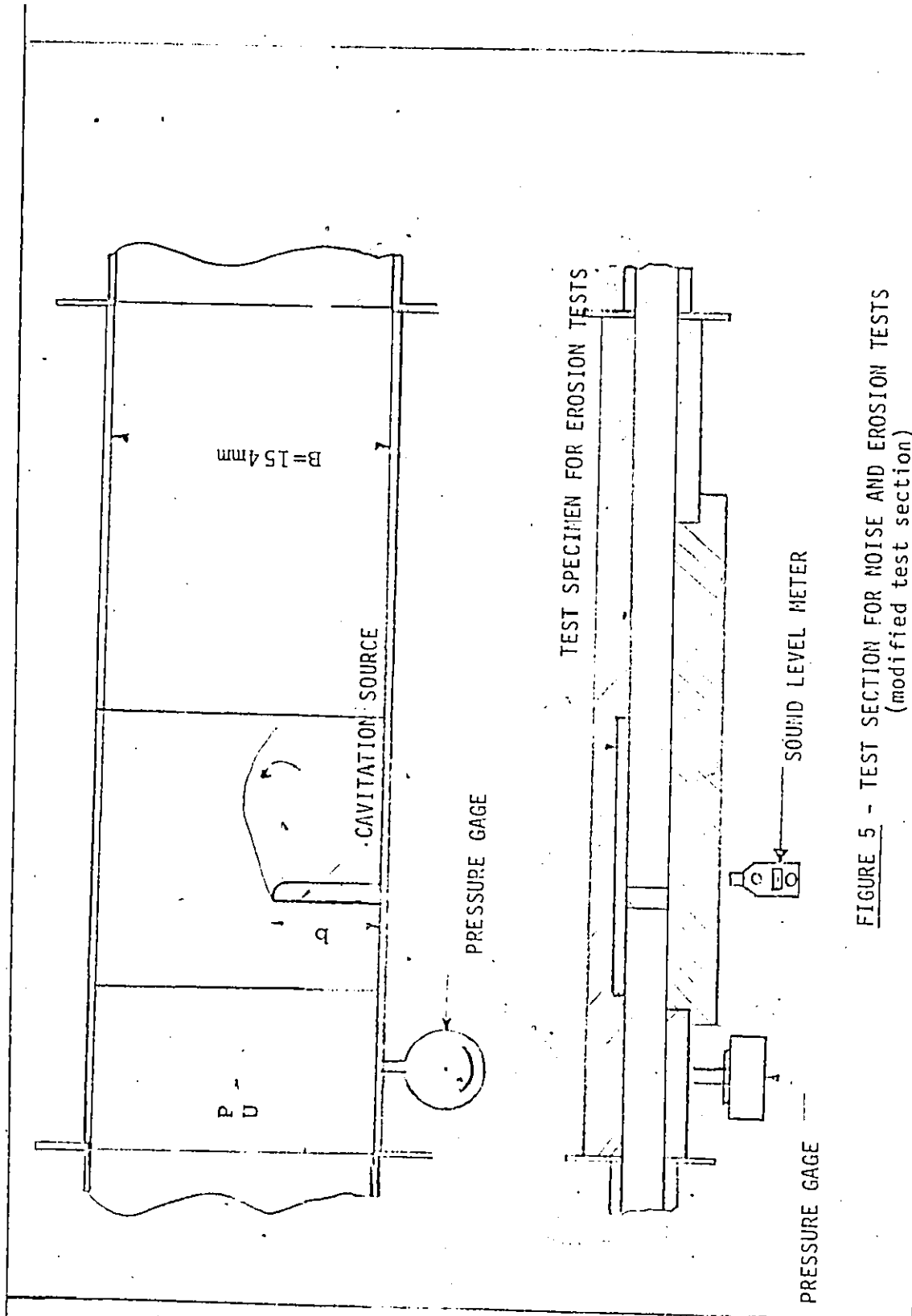


FIGURE 5 - TEST SECTION FOR NOISE AND EROSION TESTS
(modified test section)

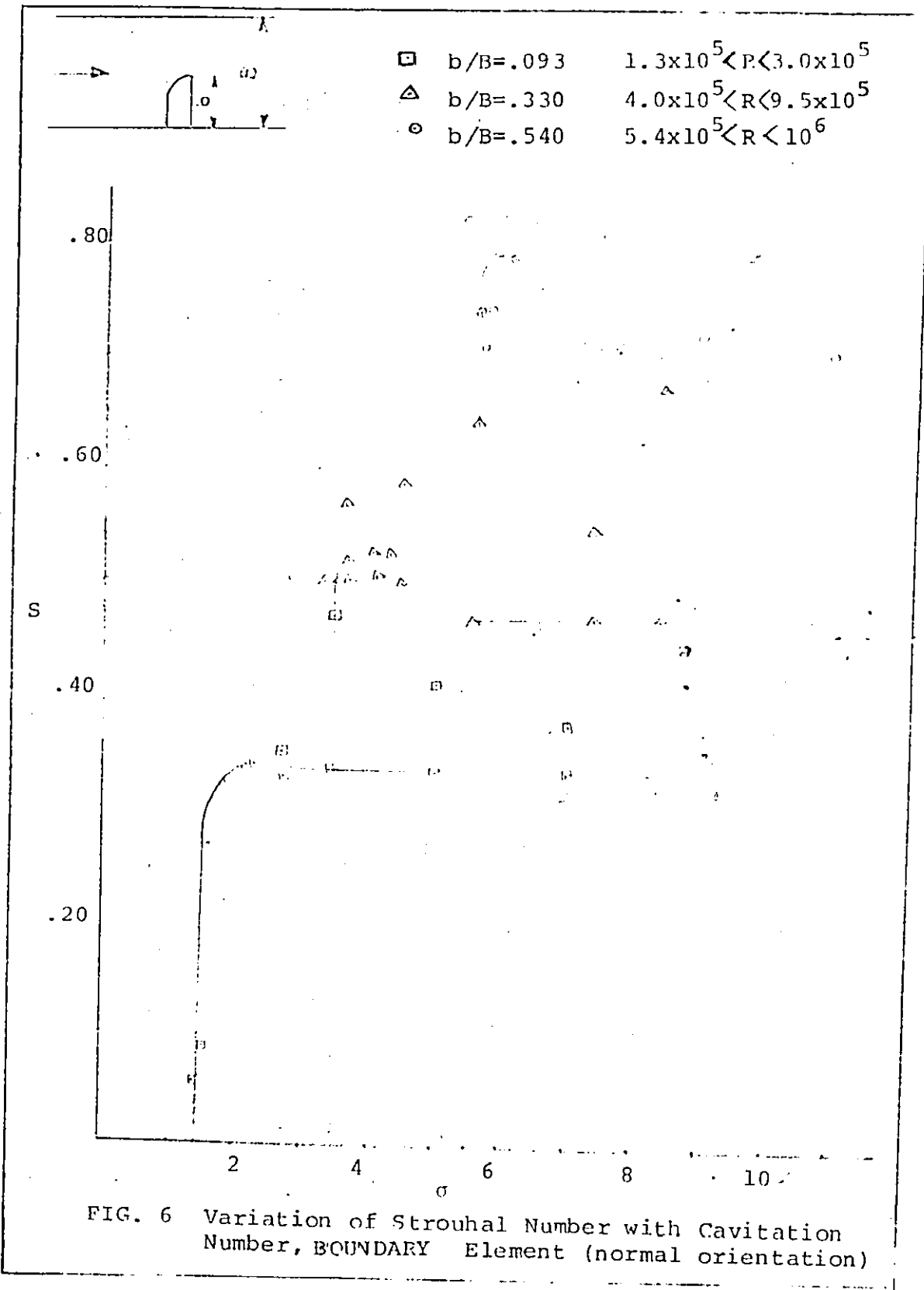


FIG. 6 Variation of Strouhal Number with Cavitation Number, BOUNDARY Element (normal orientation)

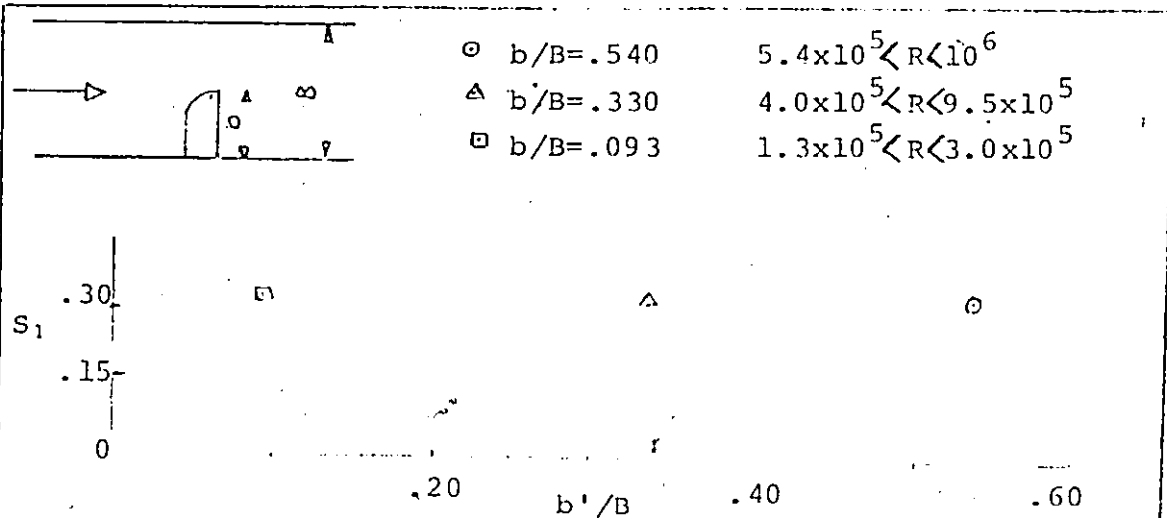


FIG. 7a Variation of Modified Strouhal Number with Blockage (non-cavitating), Boundary Element (normal orientation)

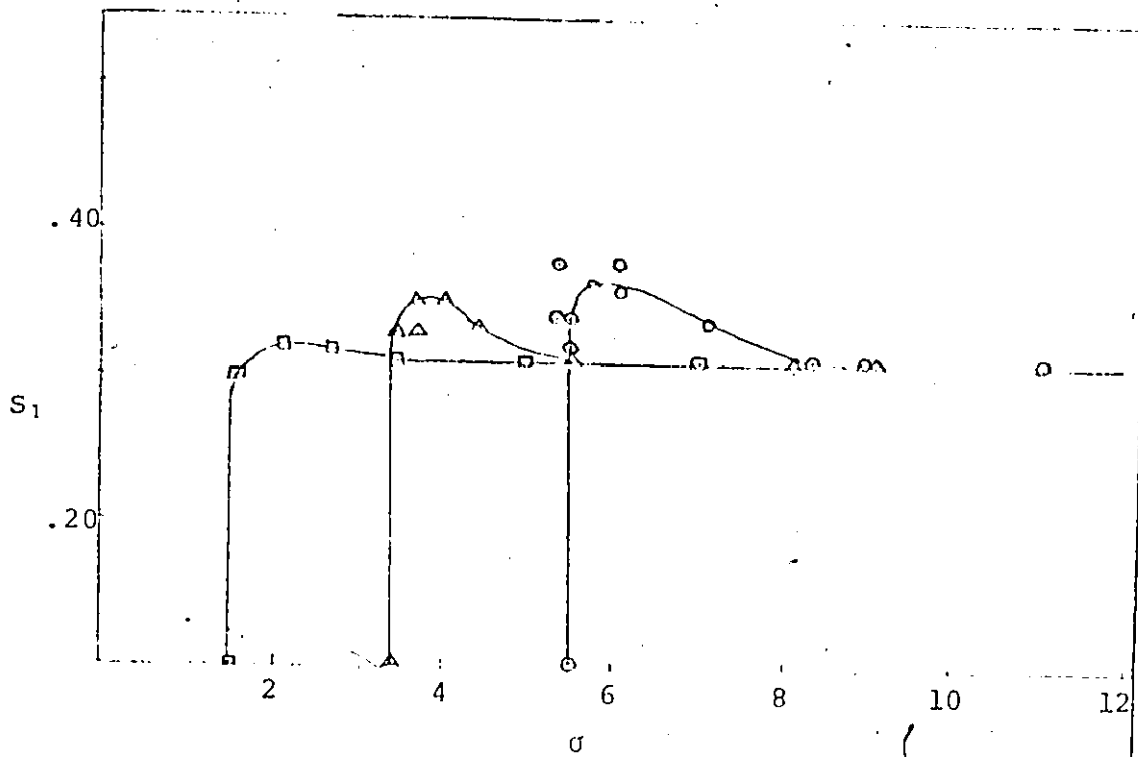


FIG. 7b Variation of Strouhal Number with Cavitation Number, Boundary Element (normal orientation)

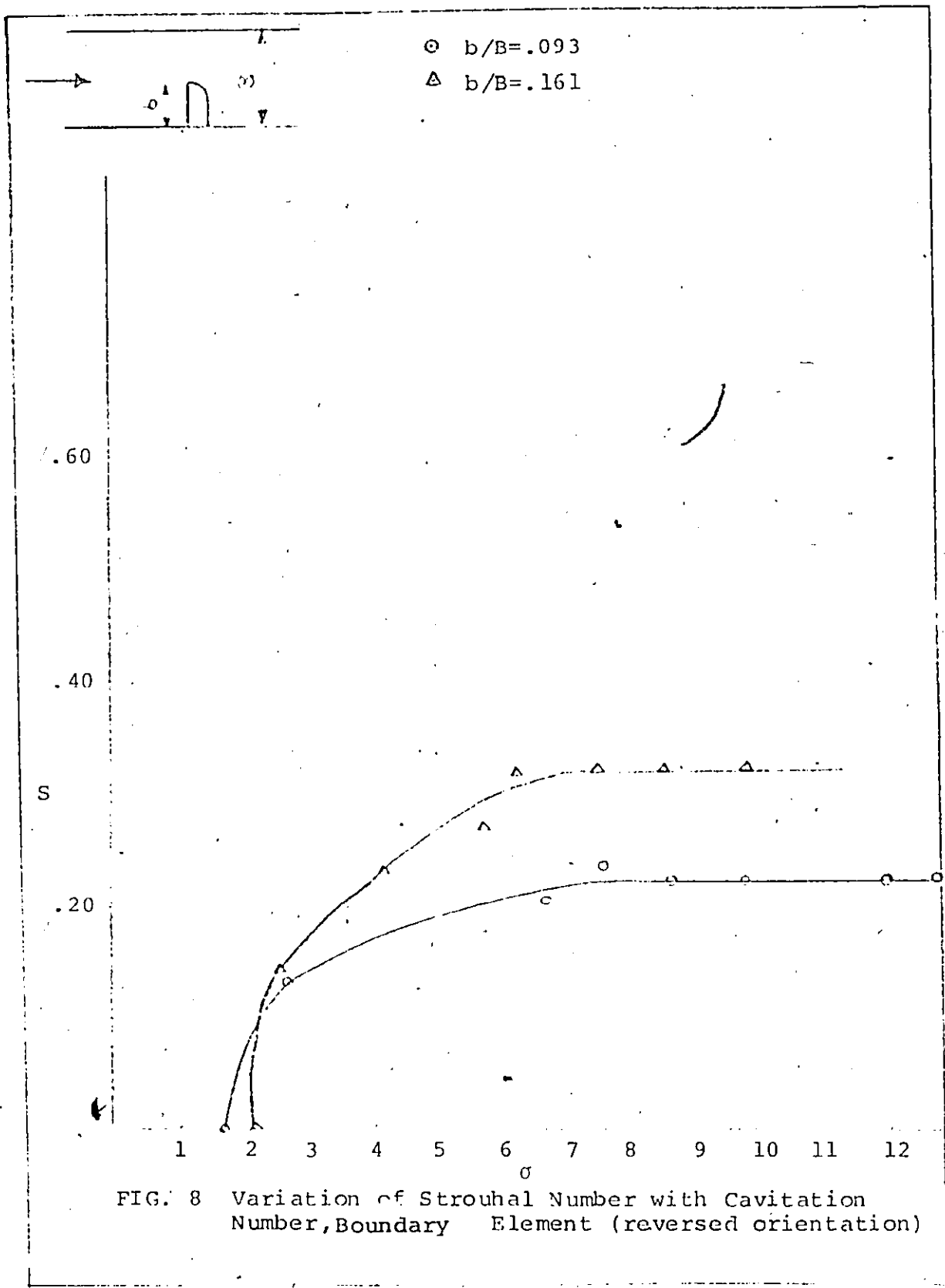
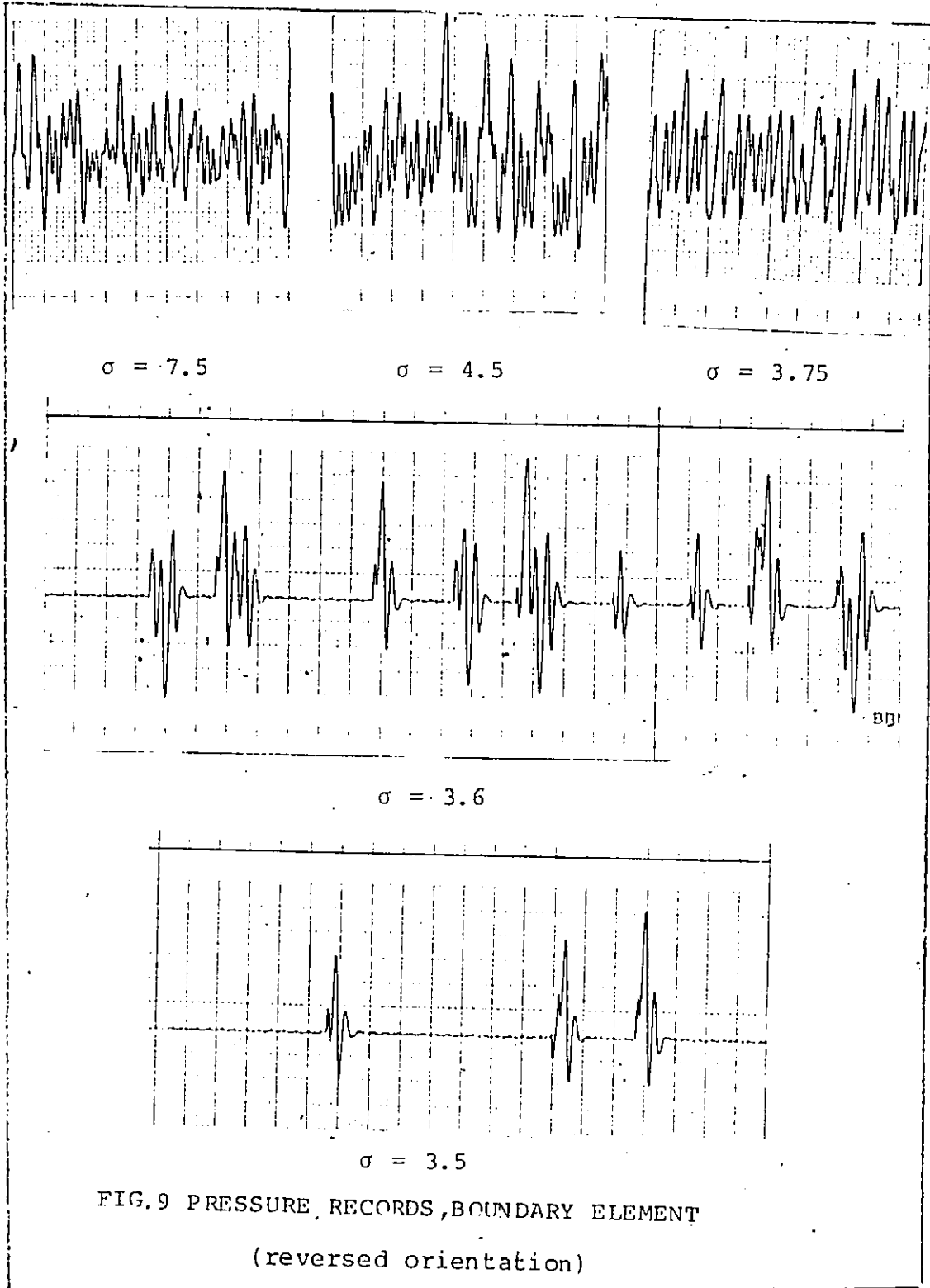


FIG. 8 Variation of Strouhal Number with Cavitation Number, Boundary Element (reversed orientation)



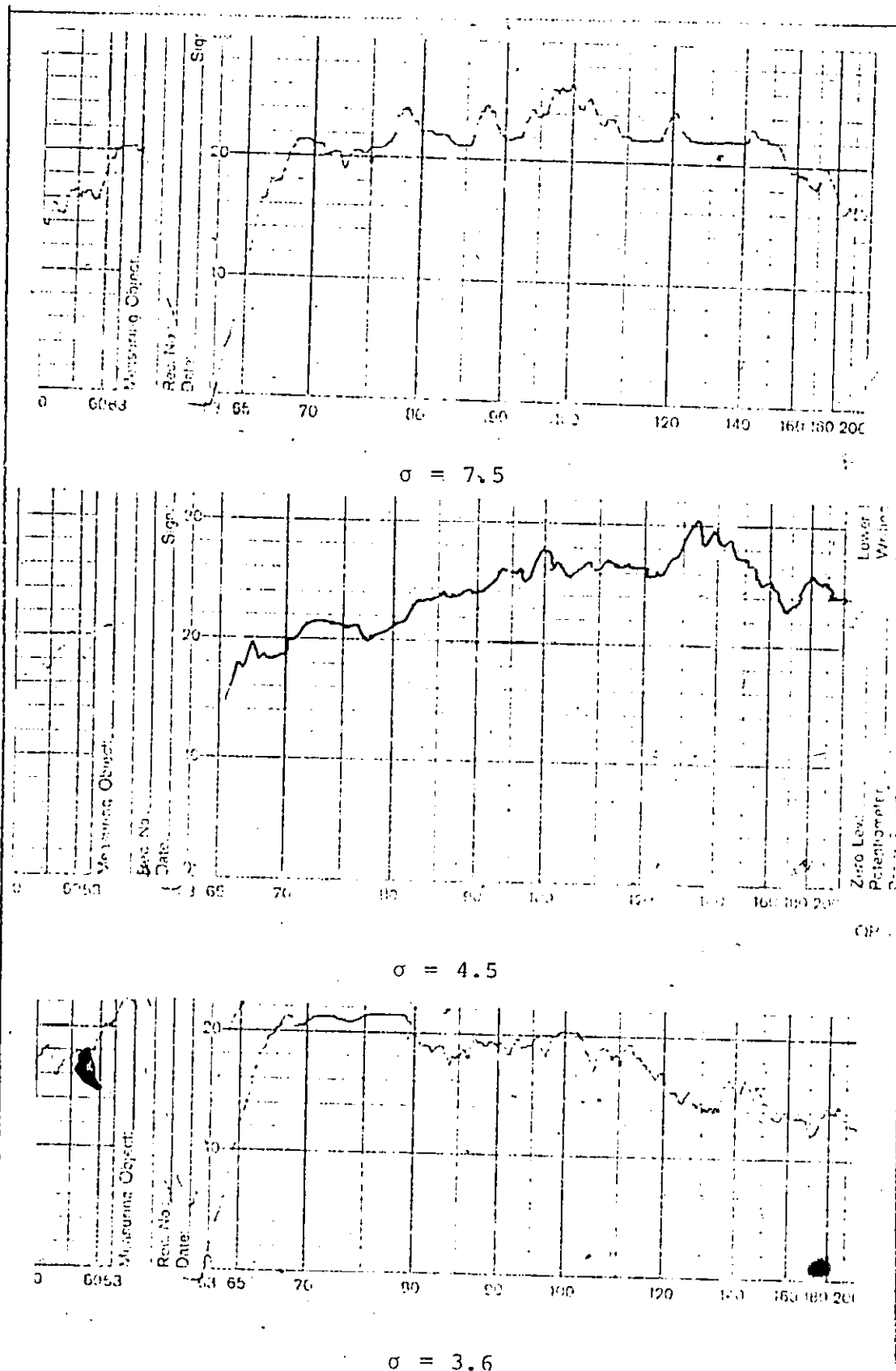
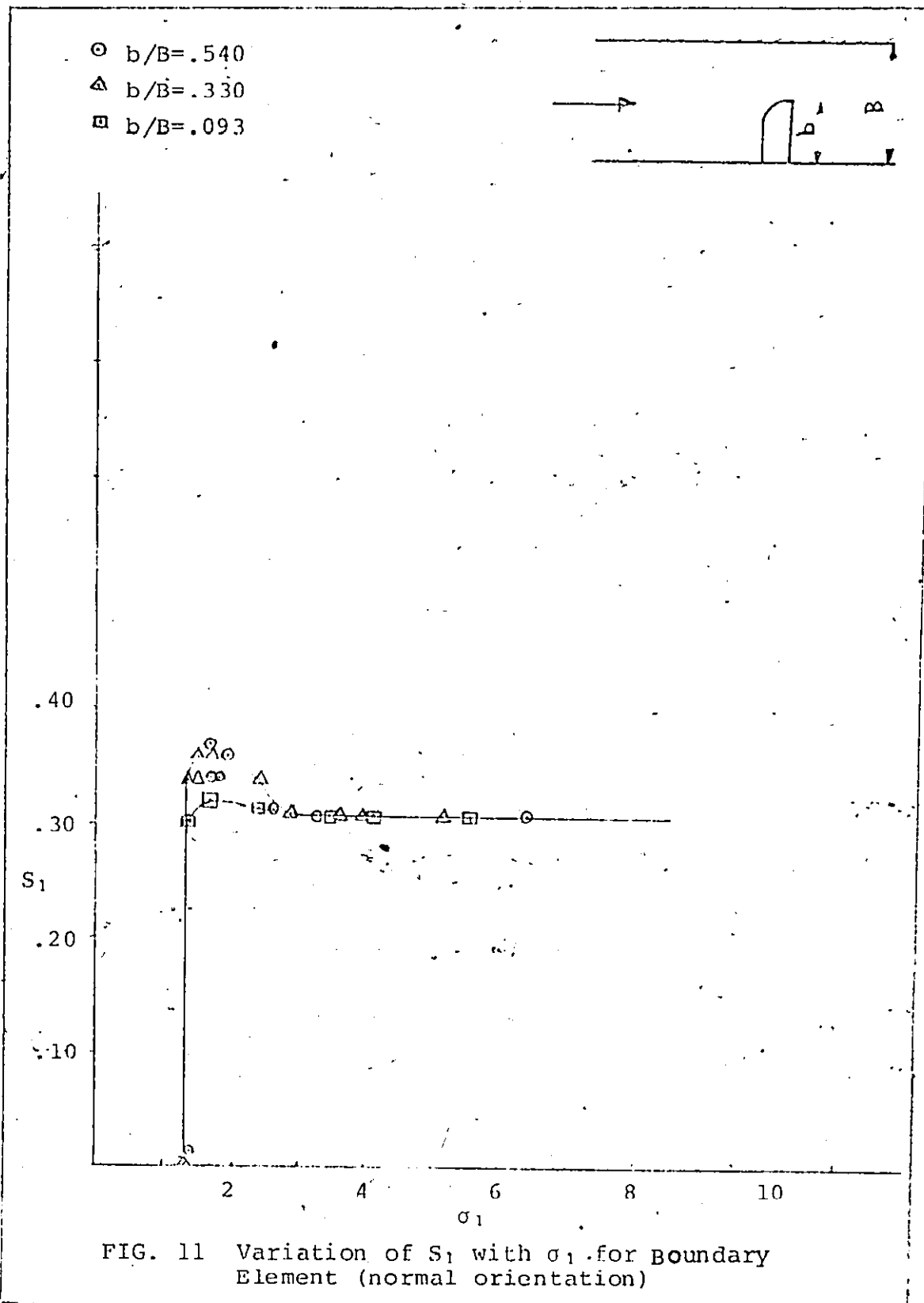


FIG.10 TYPICAL POWER DENSITY SPECTRA BOUNDARY ELEMENT
 (reversed orientation) $b/B=.33$



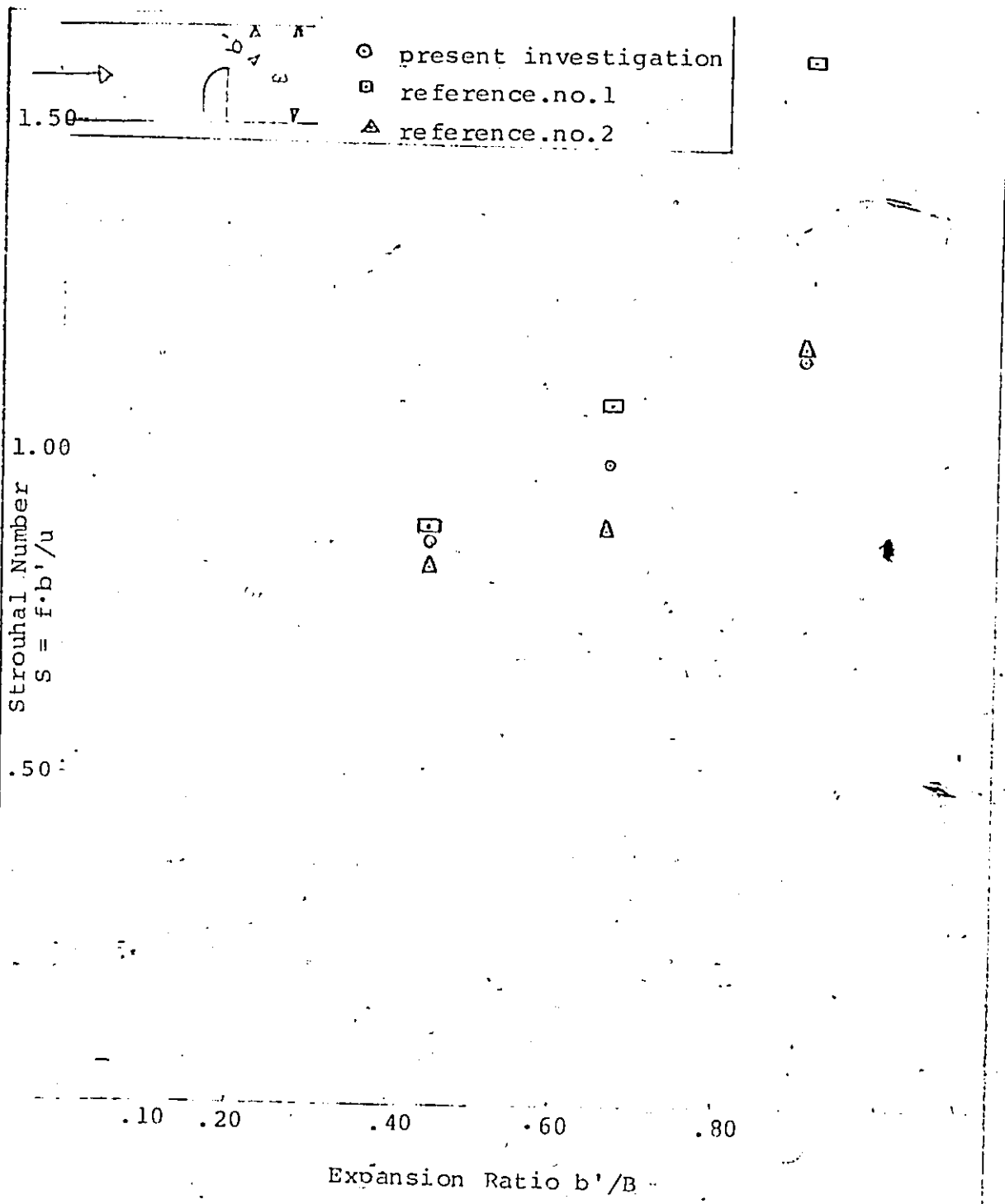


FIG. 12 Strouhal Number of Vortex Formation for Boundary Element (normal orientation)

(SEE TABLE 1)

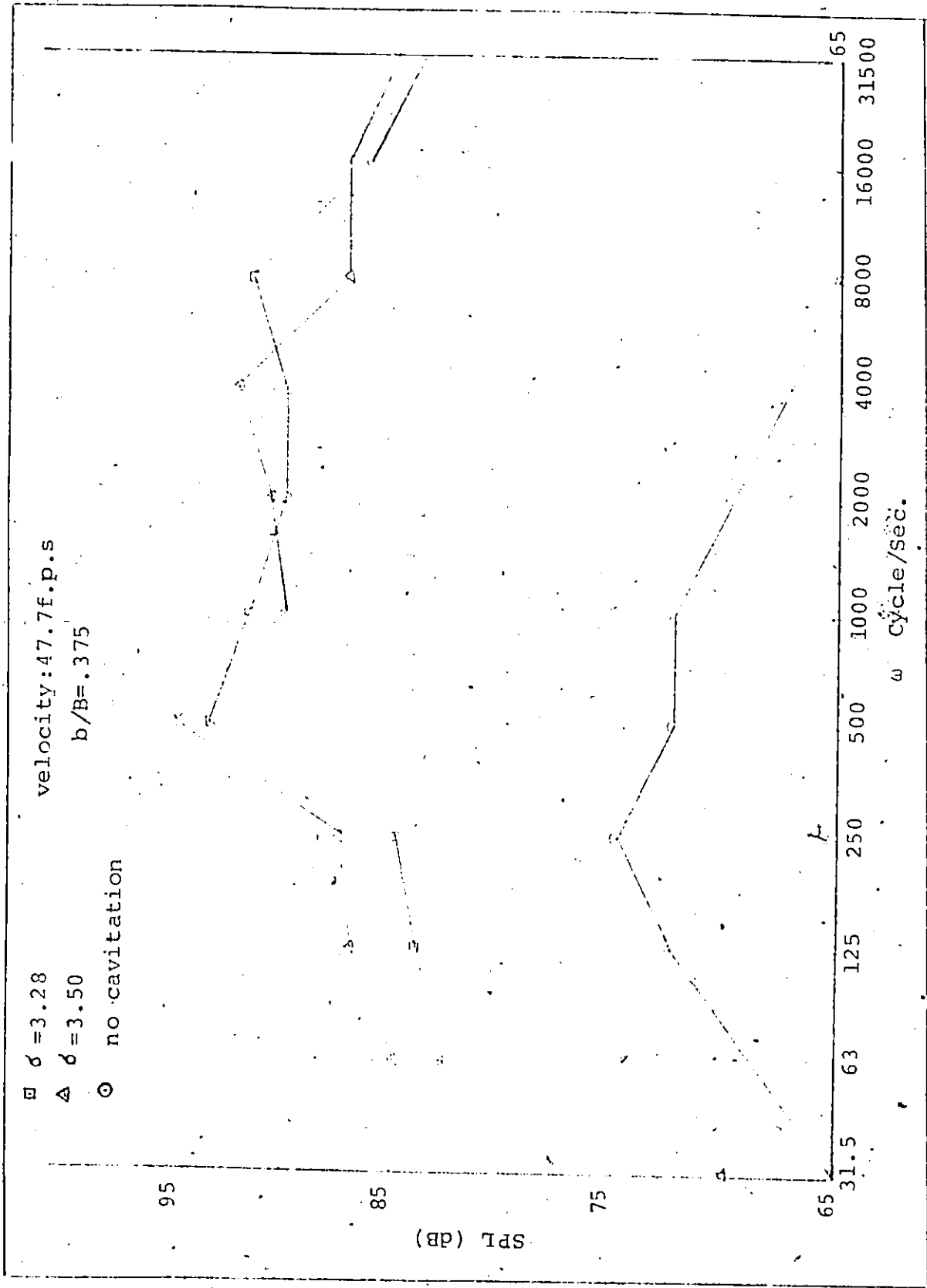
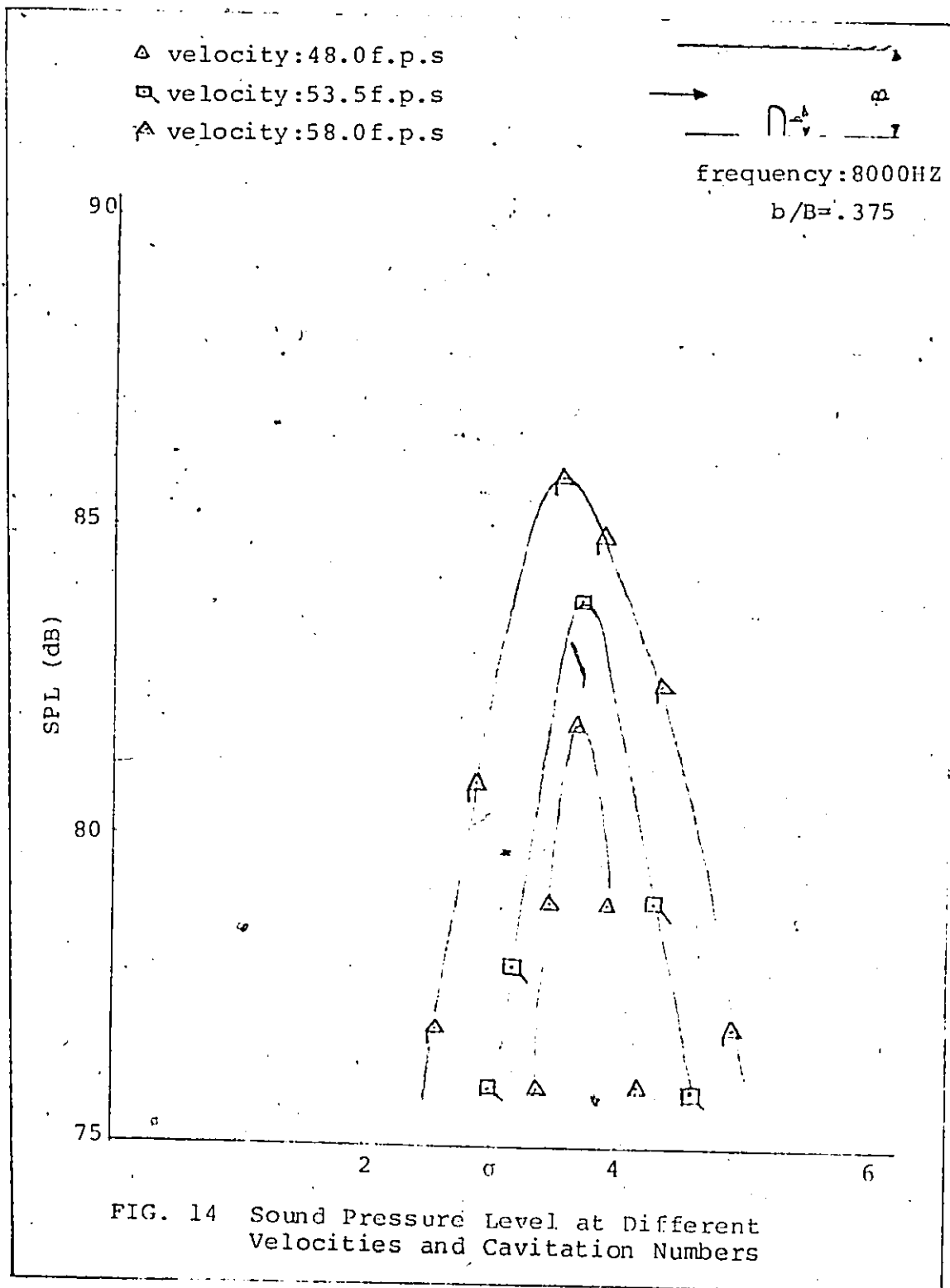


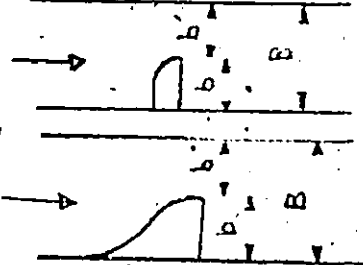
FIG. 13 Noise Spectra for Different Cavitation Numbers at Constant Velocity, Boundary Element (reversed orientation)



APPENDIX II

TABLE

TABLE 1



present investigation

ref. 1,2

ref.	b/B	$S_1 = \frac{fb}{U}$	$S_2 = \frac{2fb}{U}$	Reynolds Number
present investigation	.45	.82	1.92	$5.4 \times 10^5 < R < 10^6$
	.67	.95	1.89	$4 \times 10^5 < R < 10^5$
	.90	1.24	.27	$1.3 \times 10^5 < R < 10^5$
ref.no.1	.45	.85	1.99	
	.67	1.25	1.23	
	.90	1.85	.41	
ref.no.2	.45	.70	1.65	
	.67	.873	.86	
	.90	1.26	.28	

COMPARISON OF DATA
(see fig 12)